

# Airborne Doppler Radar Detection of Low-Altitude Wind Shear

E. M. Bracalente\*

*NASA Langley Research Center, Hampton, Virginia*

C. L. Britt†

*Research Triangle Institute, Hampton, Virginia*

and

W. R. Jones‡

*NASA Langley Research Center, Hampton, Virginia*

Using a microburst/clutter/radar simulation program, a preliminary feasibility study was conducted to assess the performance of Doppler radars for the detection of low-altitude wind shear during aircraft takeoff and landing. Preliminary results show that using bin-to-bin automatic gain control (AGC), clutter filtering, limited detection range, and suitable antenna tilt management, wind shear from a "wet" microburst can be accurately detected 10 to 65 s (.75 to 5 Km) in front of the aircraft. Although a performance improvement can be obtained at higher frequency, the baseline X-band system simulated also detected the presence of wind-shear hazard for a "dry" microburst.

## I. Introduction

LOW altitude microburst wind shear is recognized as a major hazard during takeoff and landing of aircraft. Microbursts are relatively small, intense downdrafts which spread out in all directions upon striking the ground. When such wind shear is encountered at low altitudes during landing or takeoff, the pilot has little time to react correctly to maintain safe flight. In the United States during the period 1964 to 1985, there were 26 major civil transport aircraft accidents and four incidents involving 626 fatalities and over 200 injuries for which wind shear was a direct cause or a contributing factor.

As part of its integrated wind-shear program, the Federal Aviation Administration (FAA) jointly with NASA is sponsoring a research effort to develop airborne sensor technology for detection of low-altitude wind shear during A/C (aircraft) takeoff or landing. A primary requirement for an airborne forward-looking sensor or system of sensors is to be capable of detecting both heavy ("wet") and light ("dry") precipitation microbursts. One sensor being considered for this application is microwave Doppler radar operating at X-band or higher frequency. Since absolutely clear air produces no radar return at microwave frequencies except very slight scattering from gradients in the index of refraction on the scale of the radio frequency wavelength, the emphasis in the present research is on those microbursts containing at least some liquid water.

Previous experiments<sup>1</sup> and studies have demonstrated, in a limited way, the capability of airborne Doppler radars to detect the presence of wind shear. However, for A/C landing and takeoff applications, the problems of severe ground clutter,

rain attenuation, and low reflectivity levels must be solved. To consider these problems, a microburst/clutter/radar simulation program has been developed to aid in the evaluation and development of Doppler radar concepts. The simulation program incorporates wind-field and reflectivity data bases derived from a high resolution numerical microburst model,<sup>2</sup> clutter maps derived from airborne Synthetic Aperture Radar (SAR) backscatter data, and various airborne Doppler radar configurations and signal processing concepts. The program simulates the operation of a Doppler radar located in an A/C approaching a runway, sensing signal returns from a wind shear microburst, and an airport clutter environment. A description of the microburst/clutter/radar simulation program is presented along with examples of simulation outputs.

## II. Doppler Radar Design Requirements and Performance Tradeoffs

### Preliminary Design Requirements

A preliminary set of performance requirements<sup>3</sup> has been established for design of forward-looking wind-shear detection sensors. A sensor's primary requirement is to detect severe microburst wind shear during final approach to landing (see Fig. 1) or during takeoff and to provide as a minimum 15- to 40-s (approximately 1 to 3 km) warning to the pilot. Advisory information on wind-shear conditions 50 to 100 s (4 to 8 km) in front of the A/C is also desired. The sensor or sensor system must be able to detect wind shear caused by both heavy and light precipitation microbursts. The sensor must measure mean horizontal wind speeds every 150 to 300 m out to a range of 6 to 8 km along the flight path and a small sector (approx. 20 deg) on either side of the A/C with approximately 1 m/s accuracy.

A major area of radar design that requires extensive development is the radar signal processing technique, which will suppress clutter interference and provide maximum wind-shear detection accuracy. Before these techniques can be developed and evaluated, radar parameters must be chosen and evaluated. The radar parameters chosen by the radar designer

Received Feb. 14, 1989; revision received Aug. 23, 1989. Copyright © 1989 American Institute of Aeronautics and Astronautics, Inc. No copyright is asserted in the United States under Title 17, U.S. Code. The U.S. Government has a royalty-free license to exercise all rights under the copyright claimed herein for Governmental purposes. All other rights are reserved by the copyright holder.

\*Electronic Engineer, Guidance & Control Division.

†Principal Scientist.

‡Electronic Engineer, Guidance and Control Division.

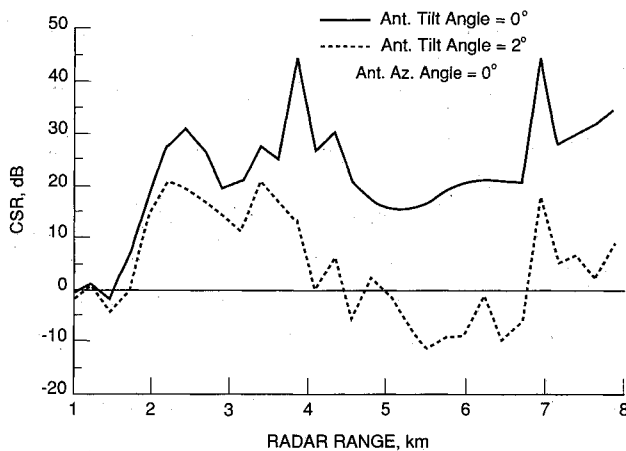


Fig. 1 Clutter-to-Signal (CSR) vs range from A/C, using Willow Run clutter map. A/C 5 km from touchdown, Ant. Az angle = 0 deg,  $Z_e = 10$  dBz. See Table 2 for other parameter values.

Table 1 Wind-shear Doppler radar parameter values

Parameter	Baseline value	Tradeoff range
Pulse repetition freq.	3030	2000-5500
Pulse width (TAU) $\mu$ -s	1.0	1.0-3.0
Max. det. range, km	10	5-10
Range gate resolution, m	150	150-450
Range sampling window, km	1-9	1-10
Max. unambiguous ws, m/s	24	24-45
Wind-speed accuracy, m/s	1.0	.5-2
Operating frequency, GHz	9.3	9.3-15
Antenna diameter, m	.76	.46-.91
Antenna gain, dB	35.5	31-48
Antenna beamwidth, deg	3	.8-5
Sidelobe level, dB	< -25	-20--35
Antenna polarization	Linear H	Dual pol
Ant. tilt angle range, deg	0-2	0-2
Azimuth angle range, deg	+/-21	+/-45
Minimum det. signal, dBz	0	-15-10
Transmitter peak power, kw	2	.2-10
System noise figure, dB	4	3-6
Return sig. dynam. range, dB	70	60-80
Receiver dynamic range, dB	50	45-55
Xmit/rec. phase jitter, d.rms	.5	.1-2
Number of A/D conv. bits	12	10-14
Clutter filter type	2 pole	TBD
Processing technique	PP	FFT, PP

are those which go in the radar equation to compute signal-to-noise ratio (SNR) performance.<sup>4</sup> The SNR for a signal reflected from a distant rain cell target is affected by a large number of parameters. The designer, however, has control over only a few of them, mainly transmitter power, antenna gain, frequency of operation, pulse duration, and to a minor degree, target range. There are, for airborne operation, a number of factors which further limit the choice of values for these parameters. The use of higher operating frequencies provides greater sensitivity to rain reflectivity and higher resolution but is subject to greater attenuation by rain. Most operational Doppler weather radars operate at frequencies of S-band (1-3 GHz), C-band (3-8 GHz), and X-band (8-12 GHz). Although negligible attenuation occurs at S-band, the increase in sensitivity and smaller cell resolution at X-band outweighs the small increase in attenuation (2-5dB) experienced for wet microbursts. For dry microbursts, frequencies in the Ku-band (12-18 GHz) region could be considered since attenuation would remain low. Wind-shear detection capability for both wet and dry microbursts could utilize dual frequency operation, but practical considerations make it desirable to find one

frequency that can provide acceptable performance for all microbursts.

Airborne weather radars operate in an allocated frequency band around 9.3 GHz and utilize solid state transmitters of about 100 watts. They are presently in use to display rain reflectivity and wind turbulence advisory information to the pilot. Therefore, it is of interest to assess airborne Doppler radar concepts for wind-shear detection operating in this frequency band utilizing relatively low power. Space limitation in the nose radome of passenger A/C limit the maximum antenna size to about 30-36 in. (0.76-0.91 m) in larger A/C and about 18-20 in. in smaller A/C. This makes it more important, from a resolution and sensitivity standpoint, to operate at the higher frequencies. It is desirable to keep transmitter power requirements low so that solid state transmitters can still be considered. Other radar parameters such as pulse repetition frequency (PRF) and pulse width are chosen to minimize velocity and range fold-over problems and to provide acceptable range resolution. Table 1 lists the range of radar parameter values being considered in the feasibility study and which represent state-of-the-art, airborne, Doppler, radar-hardware implementation capability. Also listed is a baseline set of values used in the initial radar simulation case studies.

#### SNR Performance

Using selected values of parameters found in Table 1, the SNR was computed in a bandwidth equal to the inverse of the pulse width (TAU). A SNR in this bandwidth of greater than unity (0 dB) is generally required to obtain adequate Doppler processing performance. SNR performance exceeding 0 dB can be obtained for relatively low reflectivity levels (0 to 10 dBz) for ranges out to 10 km. Reflectivity values range from 60 dBz in the core of wet microbursts to 10-40 dBz in the outflow region. The results for both the 9.3 GHz and 15 GHz indicate more than sufficient SNR performance for these ranges of reflectivities. For dry microbursts the core reflectivity can be in the range of 20 to 30 dBz, falling to -20 to +5 dBz in the outflow region. The 9.3 and 15 GHz performance for a -10 dBz reflectivity falls below 0 dB SNR at about 3 and 6 km, respectively, which are still acceptable ranges for this application. An increase in transmitter power would be required to operate down to the -20 dBz level.

#### Clutter Performance

Another major problem associated with the sensing of microbursts using an airborne Doppler radar is the presence of ground clutter. To assess the magnitude of this problem, an analysis of clutter spectra and clutter-to-signal ratios (CSR) was conducted using ground clutter maps derived from well-calibrated SAR Normalized Radar Cross Section (NRCS) data as described in Section III. A set of clutter maps has been produced for a number of different airports from existing sets of SAR data. Figures 1 and 2 show CSR results assuming a 10 dBz rain reflectivity signal level for a few sample radar configurations approaching the Willow Run, Michigan airport. Plots are shown for an A/C distance from touchdown of 5 km, antenna tilt angles of 0 and 2 deg (antenna angle measured up from the A/C glide slope of -3 deg) and antenna azimuth angles of 0 and 10 deg. Table 2 lists the radar parameters used in these analyses. Figure 3 shows a histogram plot of the range of NRCS levels which exist in the clutter map used. The NRCS levels larger than -10 dB are primarily from urban areas and high-level discrete targets.

The results of this preliminary clutter analysis show that the highest clutter levels (CSR of 30-60 dB) occur where the pulse in the main beam intersects the ground in an urban area for antenna tilt angle of 0 deg. Two significant results are shown by these analyses which can be used to greatly reduce the effects of clutter. First, lower CSR values occur at short ranges

in front of the A/C at range gates where the pulse in the main beam has not touched the ground. At these ranges the clutter is coming primarily from sidelobes, which if sufficiently low will suppress the clutter signals. Second, it is very evident in the data that a significant reduction of clutter occurs when the antenna is tilted up from 0 to 2 deg.

Thus, by limiting the range of data processing and employing proper antenna tilt control, it is felt that CSR levels can be kept below 40 dB (well within the dynamic range capabilities of present-day Doppler radar receiver design technology). High pass filtering techniques can then be employed to reduce clutter to acceptable levels. Studies are underway to evaluate filter algorithms which can provide optimum results.

### III. Radar Simulation

#### General Description

The radar simulation program is a comprehensive calculation of the expected output of an airborne coherent pulsed Doppler radar system viewing a low-level microburst along or near the approach path of the aircraft. Inputs to the program include the radar system parameters and large data files that contain the characteristics of the ground clutter and the microburst. The ground clutter data file consists of high-resolution (20 m) calibrated SAR data of selected airport areas. The microburst data files provide reflectivity factors, x, y, z wind velocity components, and other meteorological parameters with a resolution of 40 m. This data base is generated by a numerical convective cloud model<sup>2</sup> driven by experimentally determined initial conditions and represents selected time periods of the microburst development.

For each range bin, the simulation calculates the received signal amplitude level by integrating the product of the antenna gain pattern and scattering source amplitude and phase

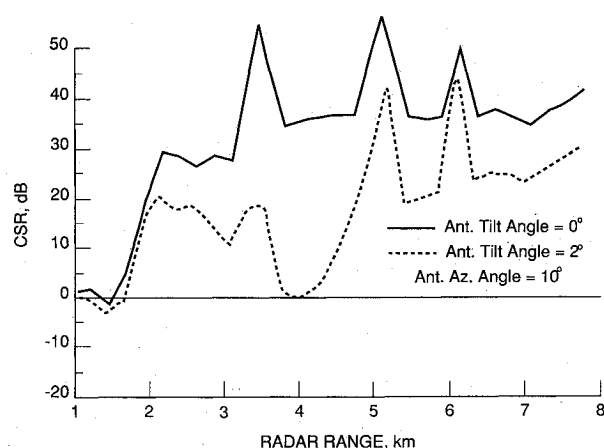


Fig. 2 Clutter-to-Signal (CSR) vs range from A/C for same conditions as Fig. 1 except Ant. Az angle = 10 deg.

Table 2 Radar parameters used in clutter analysis

A/C range from runway	5 & 7 km
A/C ground velocity	77 m/s
A/C glide slope	3 deg
Frequency	9.3 GHz
Antenna Dia.	.76 m (30 in.)
Antenna edge illum.	10 dB
Rain reflectivity	10 dBz
Pulse width	1 $\mu$ -s
PRF	5000
Ant. tilt angle	0 & 2 deg
Ant. azimuth angle	0 & 10 deg

over a spherical-shell volume segment defined by the pulse width, radar range, and ground-plane intersection. The amplitude of the return from each incremental scatterer in the volume segment is proportional to either the square root of the normalized cross section of the ground clutter (from the clutter map) or the square root of the reflectivity factor of the water droplets in the microburst (from the microburst data base). The phase of each incremental scatterer is the sum of a uniformly distributed  $(0 - 2\pi)$  random phase term, a phase term due to relative aircraft-scatterer radial velocity, and normally distributed random phase terms representing transmitter/receiver phase jitter and ground clutter random motion. The random phase terms simulating phase jitter and ground clutter motion are updated for each transmitted pulse, and the uniformly distributed phase terms are updated for each sequence of pulses in a range bin. The phase terms representing aircraft-scatterer relative motion are linear functions of time.

Path attenuation for each incremental scatterer is determined by integrating the path losses over the transmission path. Empirical formulas<sup>4</sup> are used to determine the incremental path losses from the liquid water content of the microburst. Aircraft ground velocity is assumed to be known accurately so that derived Doppler frequencies can be referenced to a value of zero corresponding to that velocity.

Antenna patterns simulated include a generic parabolic antenna with size and aperture illumination taper specified by input data and a flat plate array antenna with a pattern similar to that found in the current generation of X-band airborne weather radars.

In the simulation, a sequence of N pulses of in-phase (I) and quadrature (Q) signal amplitudes are calculated for each range bin as discussed above and subjected to automatic gain control (AGC) amplification and A/D quantization. A simulated fast-acting AGC is used to adjust the gain of the system on a bin-by-bin basis to achieve a wide dynamic range and to prevent signal saturation (due to clutter) prior to and during A/D conversion. The I and Q pulse stream is then digitally filtered to suppress ground clutter near zero Doppler frequencies and processed using both conventional pulse-pair and spectral-averaging algorithms to derive the average velocity and spectral width of the scatterers in the range bin. Further processing of the velocity data provides information on wind shear and aircraft hazard factor.

Provision is made in the simulation to generate returns from a specified number of range bins over a specified azimuth scan so that simulated color displays of reflectivity, velocity, wind shear, spectral width, etc., can be examined. Other outputs of the simulation include plots of power levels, velocity, spectral width, wind-shear hazard factor, and AGC levels vs radar range. Doppler spectra of ground clutter and moisture as

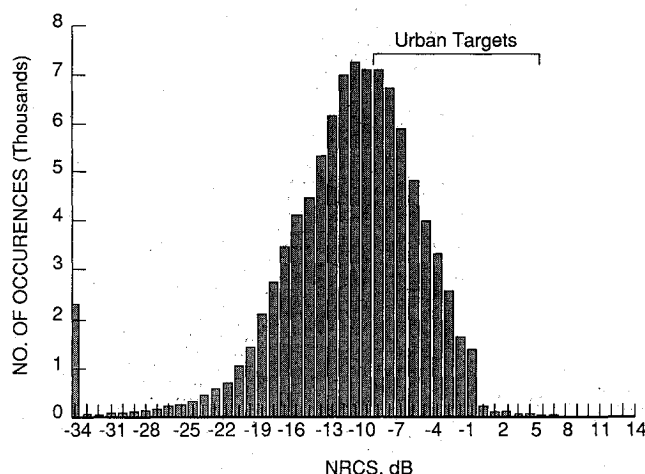


Fig. 3 Histogram plot of range of NRCS levels contained in the Willow Run Airport clutter map.

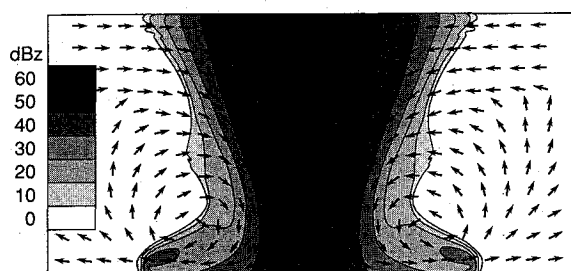


Fig. 4 Reflectivity contours and velocity field for the axisymmetric "wet" microburst model used for initial radar performance simulations studies.

derived from the I and Q signals from each simulated range bin are also plotted.

#### Microburst Model

The microburst model can be initiated from observed data and generates realistic wind fields that compare favorably with observed data such as that obtained in the Joint Airport Weather Studies (JAWS).<sup>5</sup> For the radar simulations, a  $4 \times 4$  km lattice of  $40 \times 40$  m grid spacing increments (two-dimensional axisymmetric version) has been generated at selected time periods. Output parameters include the radar reflectivity factor (dBz), wind velocity components, temperature, equivalent potential temperature, pressure, and moisture content (water vapor, ice, cloud droplets, rain, snow, and hail/graupe). The model is described in detail in Refs. 2 and 5. A three-dimensional, nonsymmetric, dry microburst similar to the one encountered by a number of aircraft landing at Denver Stapleton airport on July 11, 1988 has also been modeled and incorporated in the simulation program. Studies are underway using this model to evaluate radar performance.

For the radar simulation cases discussed in this paper, a typical wet microburst and a typical dry microburst were selected and used to investigate radar performance at a particular instant of time. Figure 4 shows the reflectivity factors and velocity field of the axisymmetric wet microburst used in the radar simulation. The dry microburst is similar in form but with smaller dimensions, lower wind speeds, and much lower reflectivity levels. The wet microburst data are taken at 11 min after initiation of the microburst calculation and the dry microburst data are 23 min after initiation. The wet microburst resembles an axisymmetric version of the August 2, 1985, Dallas-Ft. Worth storm,<sup>6</sup> and the dry microburst is based on soundings taken on July 14, 1982, within the JAWS network near Denver.

#### Clutter Model

The ground clutter model used for the present simulation cases is a high-resolution, X-band SAR map of the Willow Run, Michigan airport area provided by the Environmental Research Institute of Michigan (ERIM).

The SAR image files produced by ERIM provide calibrated NRCS data with a resolution of 20m. Figure 5 shows a high resolution (3 m) SAR image of Willow Run airport from which these data were derived and the runway (9R) used in the simulation runs. In the simulations, the aircraft is positioned at a selected distance from the runway touchdown point on a 3-deg glide slope.

A problem with the use of existing SAR data is associated with the variation of cross section with depression angle. These data were taken at depression angles ranging from approximately 18 to 50 deg; whereas for the operational airborne radar simulated, the depression angles of interest are approximately 1 to 20 deg. To partially account for this difference, ERIM supplied an empirical depression-angle correction func-

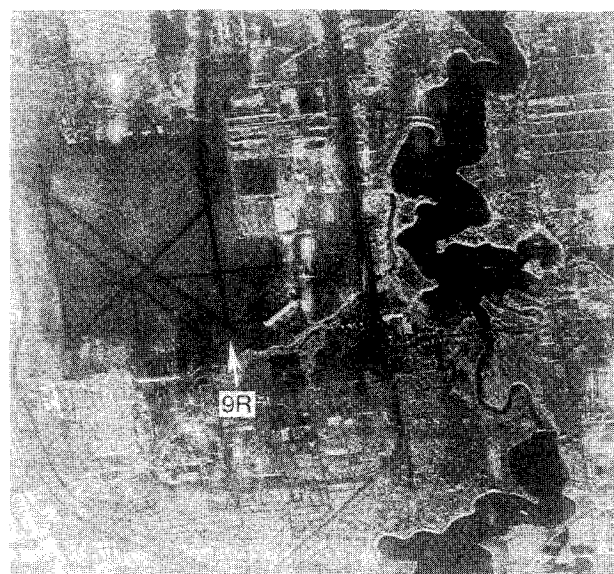


Fig. 5 High resolution SAR image of the Willow Run, MI airport area. The NRCS map, produced from this image data base, is used to calculate the ground clutter return in the radar simulation program.

tion that corrects the NRCS to the angle seen by the airborne radar. Since clutter sources from urban areas have cross sections that do not decrease significantly with depression angles in the ranges of interest, urban areas of the clutter map are excluded from this depression angle correction, and the originally measured cross-section values are used in the simulation. Also, areas of the map with NRCS values equal to or greater than 5 dB are not corrected.

The corrections for depression angle are not entirely satisfactory and cause an uncertainty in the clutter calculations of the preliminary cases discussed in this paper. Flight experiments using the ERIM SAR instrument were flown in December 1988 at the Denver, Stapleton airport. Representative airport clutter data were collected with depression angles corresponding to those that would be seen by an airborne radar on the approach path. These data provide better information of depression-angle variation of NRCS for urban environments as well as other surfaces. The processing and analysis of these data were not completed prior to the simulation studies presented in this paper. New simulation studies are now underway using an improved depression angle correction algorithm and clutter maps derived from this data.

## IV. Simulated Radar Performance

#### Wet Microburst

To examine the expected radar performance in specific situations, several cases have been simulated using the baseline system parameters given in Table 1 and the ground clutter map from the Willow Run airport area. Figure 6 plots the SNR and SCR vs radar range for a wet microburst that would be seen by the radar at a distance of 7 km from the runway touchdown point with the antenna tilted up 2 deg from the projected aircraft path. The microburst axis is located on the projected path 2 km from the touchdown point. The calculated reflectivity factor of the water droplets along a line corresponding to the projected aircraft path is also plotted in Fig. 6 for comparison to the simulated radar measurements. For this case, the SNR and SCR are high over the entire region of the microburst with a minimum value of SCR (10 dB) occurring at approximately 3 km from touchdown. This minimum value is due to high-clutter power from an urban area at this location. The SNR exceeds 20 dB over the range with approximately 18 dB difference between the near side and far side of the microburst

due to path attenuation and geometrical factors (in this plot, the power levels are not corrected for the  $R_T^2$  loss).

Figure 7 shows the calculation of the radial component of wind velocity derived from both pulse-pair and spectral-averaging algorithms operating on 128 simulated I and Q pulses from the radar. This figure also plots, for comparison, the "true" wind speed, defined as the velocity component along the center line of the antenna beam. It should be noted that the true velocity, as defined, will always differ somewhat from the radar-measured velocity because the true velocity is measured along a line (the antenna center line); whereas the radar system measures a weighted (by reflectivity and antenna pattern) average of the velocity over a finite volume of the microburst.

A two-pole, high-pass Butterworth filter was used to filter the I and Q pulses to suppress ground clutter. The 6 dB frequency response cutoff point is located at a Doppler frequency—relative to the A/C ground velocity—corresponding to a radial component of wind velocity of 3 m/s, and the filter has two zeros at zero Doppler frequency. The effect of the clutter filter can be seen in Fig. 8, which is a plot of the Doppler spectrum in a range bin 4 km from the radar calcu-

lated with and without the clutter filter. For simulated velocity measurements, a processing threshold of 4 dB is used (i.e., the pulse-pair and spectral-averaged velocities are set to zero if the radar received power is less than 4 dB greater than the noise threshold).

The simulated velocity measurements are within 2 m/s of the "true" velocity for velocities greater than 5 m/s and indicate clearly the potentially hazardous wind shear associated with the microburst. To more closely indicate the wind-shear hazard to the aircraft, a measure called the F-factor or hazard index has been defined by Bowles.<sup>3</sup> Values of F greater than 0.1 to 0.15 are considered hazardous to jet transport aircraft considering aircraft type, configuration, and range of gross weights. As shown in Fig. 9, the hazard factor reaches a maximum value of 0.1 for this microburst, and both pulse-pair and spectral-averaging algorithms give good measurements of this indicator.

#### Dry Microburst

Simulation runs similar to those discussed above were also made with the dry microburst discussed previously. Figure 10 shows the hazard index derived by these runs using the baseline system parameters operating at 9.3 GHz. The figure indicates

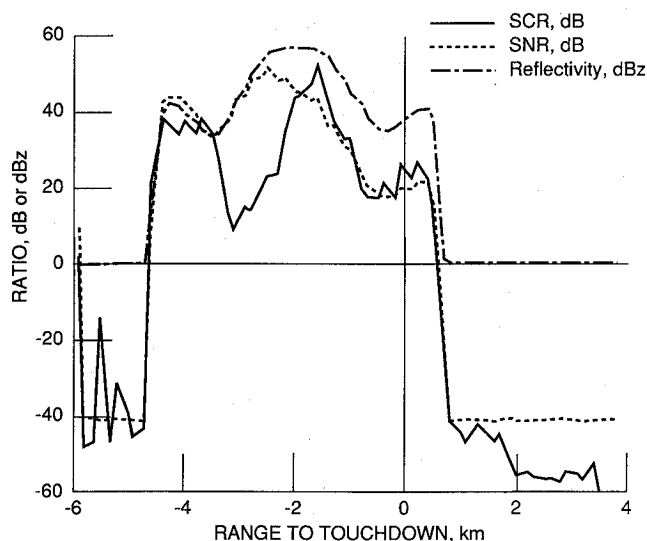


Fig. 6 Plot of calculated SNR, SCR, and reflectivity factor vs range to touchdown for the "wet" microburst. Aircraft located -7 km from touchdown on a 3 deg glide slope, radar antenna tilt = 2 deg, microburst centered on projected flight path -2 km from the touchdown point, freq. = 9.3 GHz.

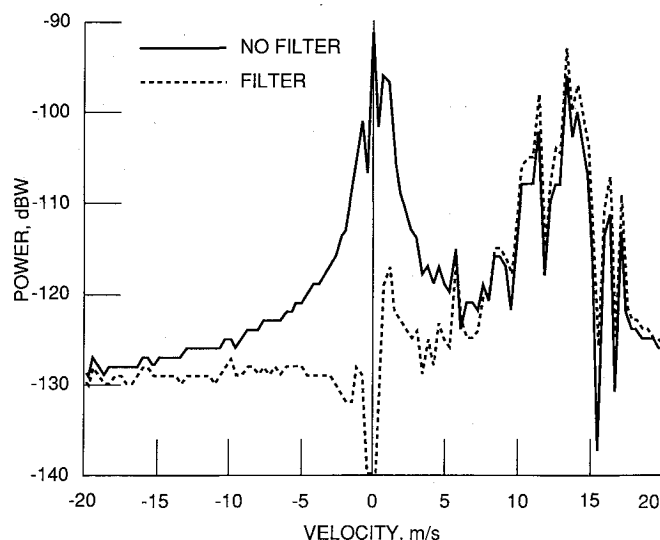


Fig. 8 Plot of Doppler spectrum from a radar range bin 4 km from touchdown, prior to wind velocity estimation, showing the effect of a 2-pole filter used to suppress ground clutter.

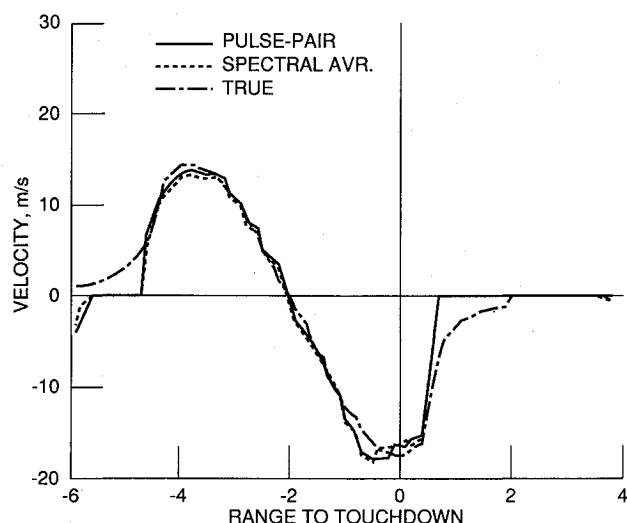


Fig. 7 Radar wind velocity measurement vs range to touchdown; same conditions as in Fig. 6. In this plot, positive velocities represent headwinds.

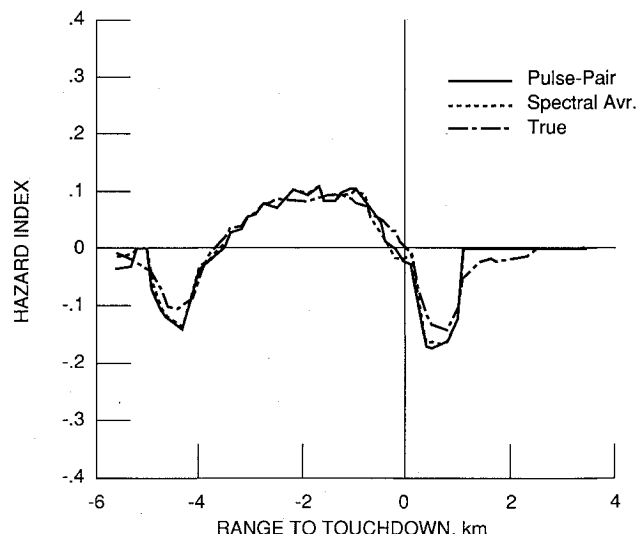


Fig. 9 Hazard index vs range to touchdown derived from the velocities shown in Fig. 7. Index is calculated from the average velocity differences over 5 range cells (750 m).

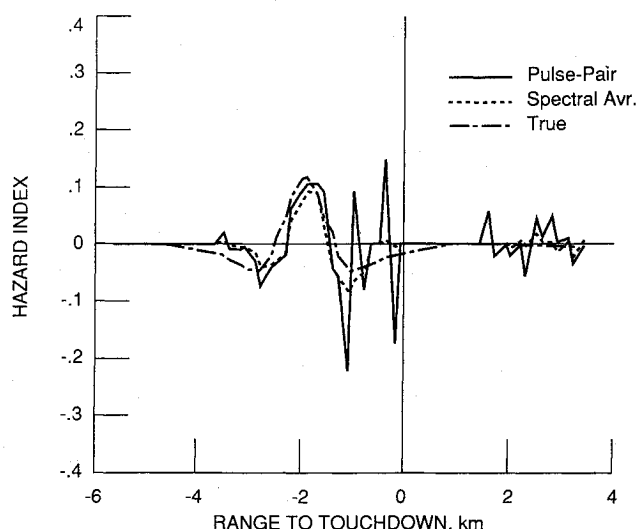


Fig. 10 Hazard index vs range to touchdown derived from the "dry" microburst velocities using the baseline parameters, and conditions listed in Fig. 6, freq = 9.3 GHz.

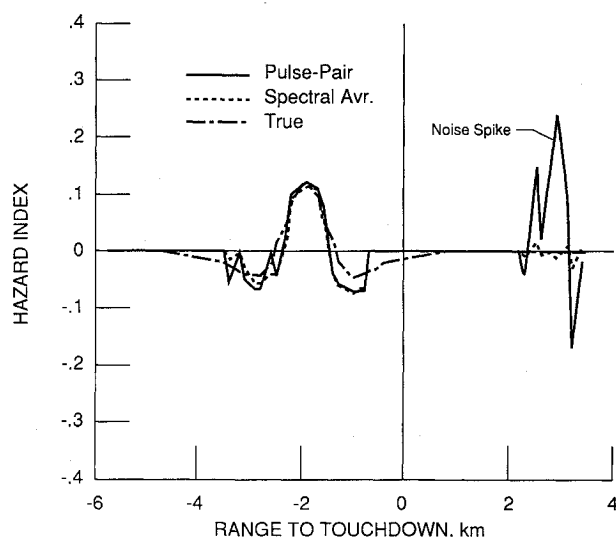


Fig. 11 Hazard index vs range to touchdown derived from the "dry" microburst velocities and conditions listed in Fig. 6, except freq. = 15 GHz and PRF = 4878 pps.

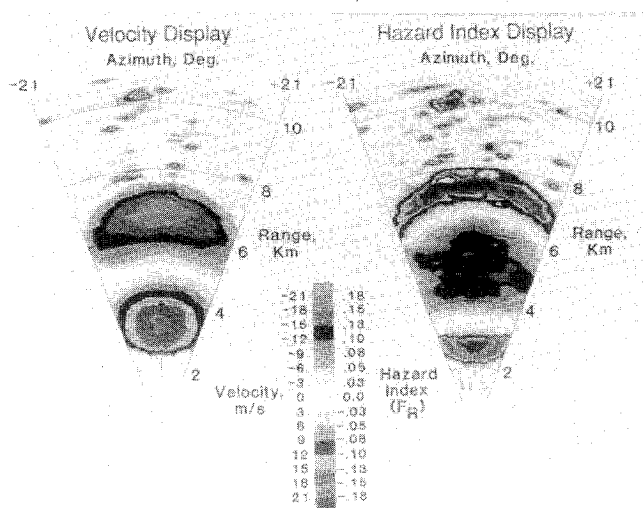


Fig. 12 Range-azimuth display of wind velocity and hazard index contours for the "wet" microburst, baseline radar parameters, and conditions listed in Fig. 6. The large head-to-tail velocity and wind direction change is clearly shown in the left display. The right display of hazard index clearly shows the potential shear hazard area.

that although the wind shear was detected, the velocity measurement with the baseline set of system parameters was somewhat noisy.

To improve the performance on the dry microburst, several system parameters can be changed. These tradeoff studies have been initiated. For example, to illustrate the radar performance at Ku-band, the dry microburst case discussed above was simulated using the same set of baseline parameters, except that the operating frequency was changed to 15 GHz and the PRF was changed to 4878 pulses per s. Preliminary results for the Ku-band system with the dry microburst indicate that even though the SNR and SCR values are much lower than those with the wet microburst, the wind velocity was successfully measured over the hazardous part of the microburst. The hazard-factor calculation (see Fig. 11) more clearly indicates the wind-shear hazard associated with this microburst.

#### Simulated Displays

The radar simulation program provides for an azimuth scan mode and the generation of simulated displays of several variables of interest. Figure 12 shows black and white copies of simulated (color) display of radial wind velocity and hazard index for the wet microburst. The left display shows contour plots of wind velocity. The right display shows the hazard index, and it clearly indicates that a potential wind-shear hazard lies on the aircraft path.

#### V. Concluding Remarks

A preliminary tradeoff and assessment study was conducted to evaluate the performance of airborne Doppler radar sensors to detect hazardous microburst wind shear during A/C landing. Using a preliminary set of performance requirements for the design of forward-looking sensors, a baseline set of radar parameters was developed for use in assessing wind-shear detection performance using a radar simulation program. This program includes excellent models of microburst wind fields, realistic clutter maps of airports, and accurate models of Doppler radar operation and signal processing.

For the baseline Doppler radar-sensor configurations modeled, preliminary analyses of the computer simulation case studies show that wind shear can be accurately detected 10 to 65 s in front of the aircraft approaching a hazardous microburst positioned in the flight path of landing aircraft. This was accomplished using a bin-to-bin AGC, clutter filtering, limited detection range, and suitable tilt management. The sensor is highly effective for the wet microburst where very high SNR and SCR are obtainable due to large reflectivity levels. For the dry microburst, with low reflectivity levels, wind shear was detected; however, more tradeoff analyses and signal processing studies are needed before the performance for the dry microburst case can be fully assessed.

Initial simulations were conducted with a specific airport, selected microburst time instants, and the baseline radar parameters. These simulations clearly show that in realistic situations, downward-looking airborne radar sensors have the potential to detect wind shear and provide information to the aircrew that will permit escape or avoidance of hazardous shear situations. Plans are underway to investigate a full range of microburst/clutter environments, conduct extensive tradeoff and optimization studies, and investigate various signal processing and clutter filtering concepts which can provide reliable wind-shear detection capability.

The initial simulation studies were confined to the landing approach since it presents the most severe signal-to-clutter situation. Studies of the takeoff case are planned. Since the antenna can be tilted up, therefore providing high signal-to-clutter ratios, acceptable detection performance is anticipated.

Although hazardous wind shear can be detected by Doppler radar, the pilot must be alerted in a timely manner to avoid the hazard. A hazard index has been developed<sup>3</sup> which establishes

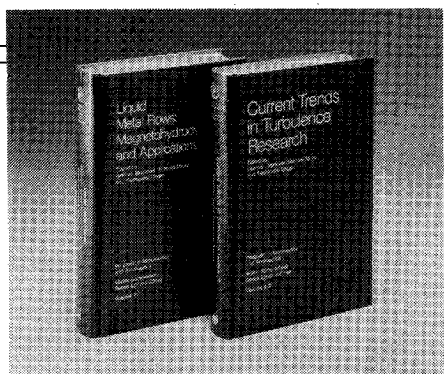
when a threat to the performance of the A/C exists. The simulation studies showed that a Doppler radar sensor can detect the horizontal component of this index with sufficient accuracy to indicate in a timely manner that a threat exists. Further studies using this index will be conducted for various microburst types and locations relative to the A/C to assess the missed and nuisance alarm rate. Displays of additional advisory information for the aircrew will probably be required and are under study. Output display examples from the simulation studies represent some of the information that could be provided.

The present and future simulation will provide a good foundation to determine the capabilities and limitations of Doppler radar concepts for the detection of microburst wind shear. Flight experiments are needed to evaluate the simulation modeling and performance estimates. A flight experiment program is planned for the 1990-93 time period. The first phase of flights will involve measuring the clutter environment from selected airports during landing approaches. These data will be used to evaluate the clutter map models derived from the SAR data. A second phase of flights will collect data from severe convective storms at altitudes above 2000 ft. The antenna will at first be kept elevated to avoid the clutter. These data will evaluate the performance of Doppler radar to detect wind

shear without the presence of clutter. Combined reflectivity and clutter data will then be collected by pointing the antenna through the storm towards the ground. These data will be used to evaluate the performance of various signal processing and clutter filtering concepts. Flight tests for candidate concept evaluation and demonstration will follow.

### References

- <sup>1</sup>Staton, L. D., "Airborne Doppler Radar For Wind Shear Detection," *Workshop Proceedings, Wind Shear/Turbulence Inputs to Flight Simulation & Systems Certification*, NASA CP 2474, July 1987.
- <sup>2</sup>Proctor, F. H., "The Terminal Area Simulation System Vol. I: Theoretical Formulation," NASA CR 4046: DOT/FAA/PM-86/50, I, April 1987.
- <sup>3</sup>Bowles, R. L., and Targ, R., "Wind Shear Detection and Avoidance: Airborne Systems Perspective," International Congress of Aeronautical Sciences, Aug-Sept 1988, Jerusalem, Israel.
- <sup>4</sup>Doviak, R. J., and Zrnic, D. S., *Doppler Radar and Weather Observations*, Academic, New York, 1984.
- <sup>5</sup>Proctor, F. H., "The Terminal Area Simulation System Vol. II: Verification Cases," NASA CR 4047: DOT/FAA/PM-86/50, II, April 1987.
- <sup>6</sup>Bowles, R. L., "Wind Shear Modeling: DFW Case Study," NASA CP 10004: DOT/FAA/PS-87/2, Oct. 1987.



## Liquid Metal Flows: Magnetohydrodynamics and Applications and Current Trends in Turbulence Research

Herman Branover, Michael Mond,  
and Yeshajahu Unger, editors

*Liquid Metal Flows: Magnetohydrodynamics and Applications (V-111)* presents worldwide trends in contemporary liquid-metal MHD research. It provides testimony to the substantial progress achieved in both the theory of MHD flows and practical applications of liquid-metal magnetohydrodynamics. It documents research on MHD flow phenomena, metallurgical applications, and MHD power generation. *Current Trends in Turbulence Research (V-112)* covers modern trends in both experimental and theoretical turbulence research. It gives a concise and comprehensive picture of the present status and results of this research.

To Order, Write, Phone, or FAX:

**AIAA** Order Department

American Institute of Aeronautics and Astronautics  
370 L'Enfant Promenade, S.W. ■ Washington, DC 20024-2518  
Phone: (202) 646-7444 ■ FAX: (202) 646-7508

V-111 1988 626 pp. Hardback	V-112 1988 467 pp. Hardback
ISBN 0-930403-43-6	ISBN 0-930403-44-4
AIAA Members \$49.95	AIAA Members \$44.95
Nonmembers \$79.95	Nonmembers \$72.95

Postage and handling \$4.50. Sales tax: CA residents add 7%, DC residents add 6%. Orders under \$50 must be prepaid. Foreign orders must be prepaid. Please allow 4-6 weeks for delivery. Prices are subject to change without notice.